

An electrode-free method of characterizing the microwave dielectric properties of high-permittivity thin films

V. Bovtun, V. Pashkov, M. Kempa, S. Kamba, A. Eremenko, V. Molchanov, Y. Poplavko, Y. Yakymenko, J. H. Lee, and D. G. Schlom

Citation: *Journal of Applied Physics* **109**, 024106 (2011); doi: 10.1063/1.3537835

View online: <http://dx.doi.org/10.1063/1.3537835>

View Table of Contents: <http://scitation.aip.org/content/aip/journal/jap/109/2?ver=pdfcov>

Published by the [AIP Publishing](#)

Articles you may be interested in

[Stress impact on dielectric properties of Bi_{3.15}Nd_{0.85}Ti₃O₁₂ films](#)

Appl. Phys. Lett. **96**, 072902 (2010); 10.1063/1.3302460

[Microwave dielectric properties of BaTiO₃ and Ba_{0.5}Sr_{0.5}TiO₃ thin films on \(001\) MgO](#)

Appl. Phys. Lett. **95**, 222902 (2009); 10.1063/1.3264051

[Structural, vibrational, and dielectric properties of a Ba_{0.5}Sr_{0.5}TiO₃ thin film: Temperature and electric field dependence from Raman spectroscopy, x-ray diffraction, and microwave measurements](#)

J. Appl. Phys. **103**, 114101 (2008); 10.1063/1.2927440

[Room-temperature tunable microwave properties of strained SrTiO₃ films](#)

J. Appl. Phys. **96**, 6629 (2004); 10.1063/1.1813641

[Structure–property relationships in pure and acceptor-doped Ba_{1-x}Sr_xTiO₃ thin films for tunable microwave device applications](#)

J. Appl. Phys. **92**, 475 (2002); 10.1063/1.1484231



You don't still use this cell phone or this computer

Why are you still using an AFM designed in the 80's?

It is time to upgrade your AFM

Minimum \$20,000 trade-in discount for purchases before August 31st

Asylum Research is today's technology leader in AFM

dropmyoldAFM@oxinst.com

OXFORD
INSTRUMENTS
The Business of Science

An electrode-free method of characterizing the microwave dielectric properties of high-permittivity thin films

V. Bovtun,^{1,a)} V. Pashkov,² M. Kempa,¹ S. Kamba,¹ A. Eremenko,² V. Molchanov,²
Y. Poplavko,² Y. Yakymenko,² J. H. Lee,³ and D. G. Schlom³

¹*Institute of Physics ASCR, Na Slovance 2, 182 21 Praha 8, Czech Republic*

²*NTUU "Kyiv Polytechnic Institute," Prospect Peremogy 37, 03056 Kyiv, Ukraine*

³*Department of Materials Science and Engineering, Cornell University, Ithaca, New York 14853-1501, USA*

(Received 16 November 2010; accepted 4 December 2010; published online 20 January 2011)

A thin dielectric resonator consisting of a dielectric substrate and the thin film deposited upon it is shown to suffice for microwave characterization and dielectric parameter measurement of high-permittivity thin films without electrodes. The $TE_{01\delta}$ resonance mode was excited and measured in thin (down to 0.1 mm) rectangular- or disk-shaped low-loss dielectric substrates ($D \sim 10$ mm) with permittivity $\epsilon' \geq 10$ inserted into a cylindrical shielding cavity or rectangular waveguide. The in-plane dielectric permittivity and losses of alumina, $DyScO_3$, $SmScO_3$, and $(LaAlO_3)_{0.29}(SrAl_{1/2}Ta_{1/2}O_3)_{0.71}$ (LSAT) substrates were measured from 10 to 18 GHz. The substrate thickness optimal for characterization of the overlying thin film was determined as a function of the substrate permittivity. The high sensitivity and efficiency of the method, i.e., of a thin dielectric resonator to the dielectric parameters of an overlying film, was demonstrated by characterizing ultrathin strained $EuTiO_3$ films. A 22 nm thick $EuTiO_3$ film grown on a (100) LSAT substrate and strained in biaxial compression by 0.9% exhibited an increase in microwave permittivity at low temperatures consistent with it being an incipient ferroelectric; no strain-induced ferroelectric phase transition was seen. In contrast, a 100 nm thick $EuTiO_3$ film grown on a (110) $DyScO_3$ substrate and strained in biaxial tension by 1% showed two peaks as a function of temperature in microwave permittivity and loss. These peaks correspond to a strain-induced ferroelectric phase transition near 250 K and to domain wall motion. © 2011 American Institute of Physics. [doi:10.1063/1.3537835]

I. INTRODUCTION

Thin dielectric layers with high dielectric permittivity ($\epsilon' > 100$) and low or moderate losses ($\tan \delta < 0.1$) belong to the basic elements of the microwave (MW) integrated circuits, multilayer heterostructures and metamaterials. Ferroelectric (FE) films deposited on a substrate provide practical realization of the mentioned structures and therefore meet widespread applications as on-chip capacitors, voltage tunable capacitors for frequency agile resonant filters and MW phase shifters for steerable antennas, etc. (see, for instance, Refs. 1 and 2). Modeling, simulation and design of MW devices need an exact value of the film ϵ' and $\tan \delta$ obviously measured at MWs. MW dielectric properties of FE films are also important for better understanding of their polarization and losses mechanisms. Low-frequency dielectric properties are essentially influenced by defects and mesoscopic inhomogeneities of the crystal structure like domains and grains while the MW dielectric properties reflect mainly fundamental polarization mechanisms caused by crystal lattice dynamics.^{2,3}

So, MW characterization of thin FE films is an actual problem important for materials physics, research, development, and application. Unfortunately, electrode structures on the top of films, as well as the bottom electrode between the film and substrate influence the measured film parameters

due to the change in properties of the near-electrode interfacial layers and to the imperfect conductivity of the electrodes.⁴ To avoid the problem and receive the intrinsic dielectric properties of the film, one should look for the MW methods which can be realized without electrodes at the film surface. The extended cavity perturbation technique⁵ was proposed for dielectric films deposited on low-permittivity ($\epsilon' = 2 \div 4$) dielectric substrates. Recently we reported application of the nonresonance waveguide method⁶ and composite dielectric resonator (DR) (Ref. 7) for the electrode-free thin film measurements. The $TE_{01\delta}$ composite DR (Ref. 7) easily includes the film on a substrate as a part of the resonance system and its parameters were shown to be sensitive to the thin film dielectric properties. Electric field in the film and substrate has only in-plane components and therefore influence of the film-substrate interface on dielectric properties is minimized.

In this work we improve the composite DR method. Composite DR described in Ref. 7 consists of three components as follows: base DR, substrate, and film. The film volume fraction is very low and provides a small shift of the DR resonance frequency; only a few MHz (megahertz). To increase sensitivity of the composite DR to the film and simplify the DR structure, we propose to remove the base component and measure the thin DR which consists only of the substrate and thin film. This approach looks realistic at least for the low-loss substrates with $\epsilon' \geq 10$, where the well de-

^{a)}Electronic mail: bovtun@fzu.cz.

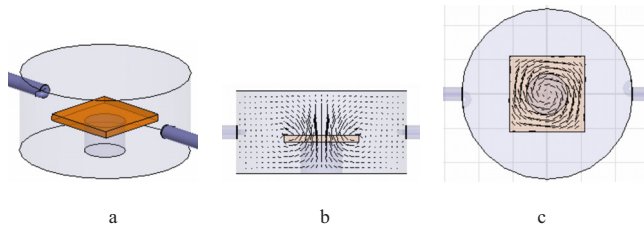


FIG. 1. (Color online) Thin DR in the cylindrical shielding cavity: scheme of the measuring cell (a), magnetic (b) and electric (c) field distribution for the $TE_{01\delta}$ resonances (marked as TE peaks in Fig. 2).

finer dielectric resonance is assured. Accounting usual substrate diameter ($D \sim 10$ mm) and thickness ($L = 0.1 \div 1$ mm), the thin DR is characterized by the ratio $L/D = 0.01 \div 0.1$ which is essentially lower than $L/D = 0.3 \div 0.6$ optimal for the $TE_{01\delta}$ DR.⁸ Can the $TE_{01\delta}$ mode be excited in such a thin DR? Which substrate thickness is optimal for the thin films measurements? Can the method sensitivity be improved? In our study we answer these questions experimentally and demonstrate efficiency of the thin DR method for the MW characterization of thin FE films.

II. CHARACTERIZATION OF THIN LOW-LOSS DIELECTRIC SUBSTRATES

First, dielectric substrates were studied as thin DRs. Rectangular dense alumina (Al_2O_3 , $\epsilon' = 9.5$) substrates (side dimensions $a = b = 10$ mm) with different thickness (from 0.3 to 1 mm) were prepared and combined to create DRs with thickness from 0.3 to 6 mm. These DRs were measured in the cylindrical shielding cavity using the transmission setup with a weak or moderate coupling^{8,9} by Agilent E8364B network analyzer. DRs (substrates) were placed on the quartz support at the coupling loop level [see the scheme in Fig. 1(a)]. Spectra of the transmission coefficient S_{21} include beside DR resonances also cavity resonances and hybrid modes (Fig. 2). Nevertheless, the $TE_{01\delta}$ mode was certainly identified by analysis of the continuous shift of the resonance frequency with the decrease of DR thickness (Fig. 3). Experimental resonance frequencies correspond well to those calculated for the $TE_{01\delta}$ mode of the cylindrical alumina DRs with $\epsilon' = 9.5$ and an effective diameter $D = 10.82$ mm using

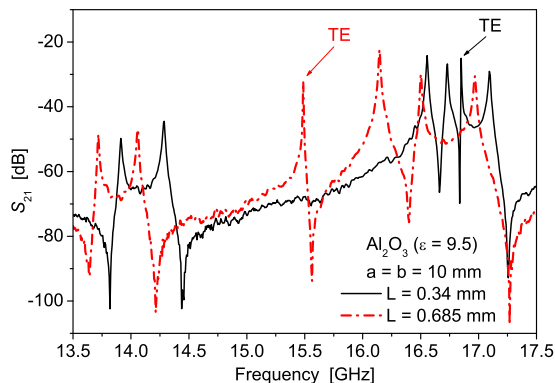


FIG. 2. (Color online) Transmission coefficient spectra for alumina substrates with different thickness. Denoted TE peaks correspond to the $TE_{01\delta}$ resonances.

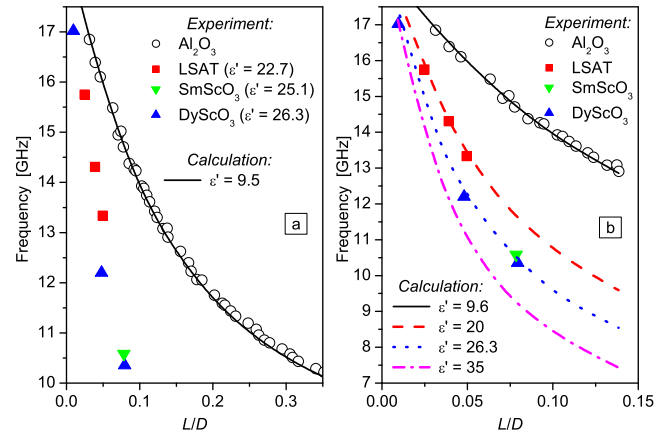


FIG. 3. (Color online) $TE_{01\delta}$ resonance frequencies of rectangular alumina, $DyScO_3$, and $SmScO_3$ substrates ($a = b = 10$ mm), as well as a disk ($D = 10$ mm) LSAT substrate in the shielding cavity in dependence on the L/D ratio. Symbols correspond to the experimental resonance frequencies, lines show the frequencies calculated in accordance with (Refs. 8 and 9) (a) or simulated by the ANSOFT HFSS software (b) accounting permittivity values denoted in the figure.

the electrodynamic analysis.^{8,9} The effective diameter D of our rectangular DRs was determined by the approximate formula as follows:¹⁰

$$D = \frac{1.53 \cdot a \cdot b}{\sqrt{a^2 + b^2}}, \quad (1)$$

where a and b are side dimensions of the rectangular DR. In our case $a = b = 10$ mm. The formula (1) was derived by comparison of cylindrical and rectangular $TE_{01\delta}$ DRs having equal thicknesses, resonance frequencies and transversal wave numbers. Simulation of the electromagnetic field distribution in our resonance system by the ANSOFT HFSS software¹¹ also proves the $TE_{01\delta}$ type of the selected resonance mode [see Figs. 1(b) and 1(c)]. Single crystal rectangular ($a = b = 10$ mm) or disk ($D = 10$ mm) substrates (110) $DyScO_3$, (110) $SmScO_3$, (100) LSAT [i.e., $(LaAlO_3)_{0.29}(SrAl_{1/2}Ta_{1/2}O_3)_{0.71}$] with an averaged in-plane permittivity $\epsilon' = 26.3, 25.1, 22.7$, respectively, and a thickness from 0.1 to 0.8 mm were also measured (Fig. 3). In this way the very low geometric factors $L/D = 0.01 - 0.02$ were achieved.

We should note that numerical calculations based on the electrodynamic analysis,^{8,9} even if it was not initially intended for such thin DRs, work well down to $L/D = 0.01$ and could be used as a first approach for estimation of substrate dielectric parameters from the thin DR measurements. Even in the case of the approximate representation of rectangular DRs as the effective cylindrical ones by formula (1), obtained dielectric parameters coincide well with the nominal ones. It is demonstrated both by a good agreement of the experimental and calculated results in Fig. 3 and by the temperature dependences of dielectric permittivity, loss (ϵ'') and $\tan \delta$ of some substrates (Fig. 4) measured in a Sigma System M18 temperature chamber (100–380 K). Also the structural phase transition in LSAT (Ref. 12) is clear evidenced by the small permittivity anomaly and dielectric loss maximum

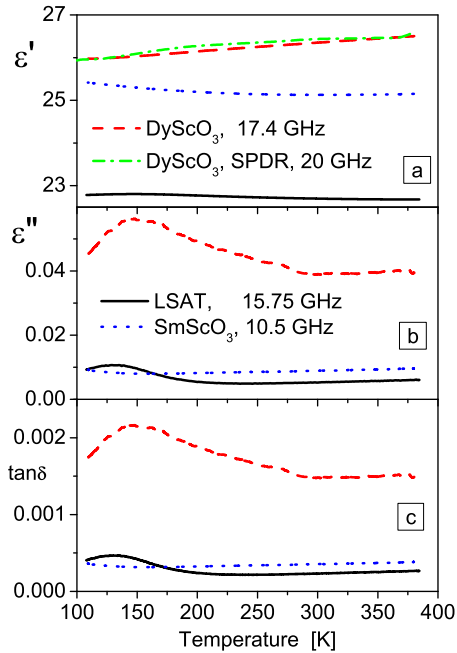


FIG. 4. (Color online) Temperature dependences of the averaged in-plane dielectric permittivity (a), loss (b), and $\tan \delta$ (c) of the (110) DyScO₃, (110) SmScO₃, and (100) LSAT substrates measured by thin DR (dashed-dotted line presents results of the split-post DR measurements).

near 150 K. Similar values of dielectric parameters were obtained in the DyScO₃ substrates by thin DR and split-post DR (Ref. 9) techniques [Fig. 4(a)].

So, very thin dielectric substrates, down to 0.1 mm in the case of $\epsilon' > 10$, could be successfully measured using TE_{01δ} DR. It is very important for the measurements of thin films deposited on the substrate; increase in the film/substrate thickness ratio results in the increase in the method sensitivity. It is even more important in the case of single crystal substrates which are mainly used to obtain FE films with a biaxial tensile or compressive mechanical strain.¹³ The strain is relaxed in the case of thick films (above 100 nm thickness). Therefore, the very thin (20–100 nm) incipient FE films (SrTiO₃, EuTiO₃, etc.) are of interest.¹⁴ Consequently, the thin substrate is preferable to ensure the method sensitivity.

The optimum substrate thickness should also provide the TE_{01δ} resonance well separated from other ones, to avoid their influence on the measured values of resonance frequency (F_R) and quality factor (Q_0). According to both calculations and experiments, the TE_{01δ} resonance separation can be easier achieved for the thin DR inserted in a rectangular waveguide where S_{21} spectra are free from the cavity resonances and only separation from the nearest HE_{11δ} resonance remains as a main problem. Usually, the TE_{01δ} resonance frequency is the lowest one, but for thin DRs ($L/D < 0.2$ in Fig. 5) the HE_{11δ} resonance frequency shifts below the TE_{01δ} one (Fig. 5). The same behavior takes place also in the shielding cavity, only the resonance frequencies are somewhat lower. Identification of the TE_{01δ} and HE_{11δ} resonances for thin DRs allowed us to estimate of the optimum DR thickness for the sufficient TE_{01δ} resonance separation accounting also the cavity resonances. This thickness de-

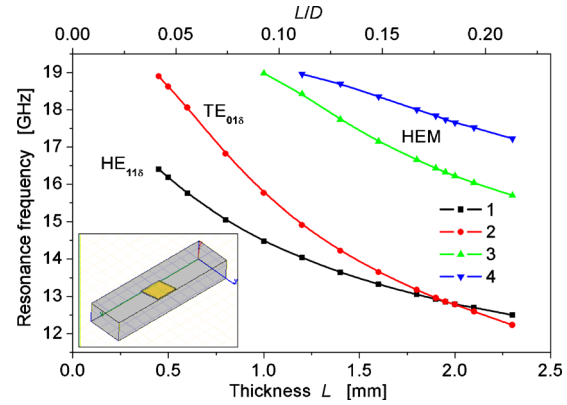


FIG. 5. (Color online) Thickness dependences of the HE_{11δ} (1), TE_{01δ} (2), and mixed HEM [(3) and (4)] resonance frequencies of the rectangular DRs ($a=b=10$ mm) with $\epsilon'=10$ in the K_u-band rectangular waveguide (insertion)

pends on the substrate permittivity and cavity size and construction. For our shielding cavity, $L=0.65\text{--}0.85$ mm is the optimum thickness for alumina (Fig. 2) or sapphire substrates ($\epsilon'=9\text{--}11$) while $L=0.2\text{--}0.3$ mm for single crystal substrates ($\epsilon'=22\text{--}27$). The separation of the TE_{01δ} resonance can be also achieved or improved by an adjustment of the cavity height or support size.

III. CHARACTERIZATION OF THIN HIGH-PERMITTIVITY FILMS

Being able to measure dielectric parameters of the thin substrate, we can determine dielectric parameters of the film in the way described for the composite DR in Ref. 7 but without any base component. We studied compressively and tensile biaxially strained EuTiO₃ films. Bulk EuTiO₃ is the incipient FE (Ref. 15) but it was theoretically proposed¹⁶ and experimentally confirmed¹⁷ that the strained EuTiO₃ thin films can exhibit the FE order. A 22 nm thick EuTiO₃ film grown on a (100) LSAT substrate and strained in biaxial compression by 0.9% was characterized in the following way. Two LSAT substrates identical in size ($D=10$ mm, $L=248$ μm) without and with deposited film were measured as TE_{01δ} DRs in a shielding cavity which is more convenient for realization of temperature measurements comparatively to the waveguide setup. Temperature dependences of the TE_{01δ} resonance frequencies and quality factors shown in Figs. 6(a) and 6(b) were used to calculate temperature dependences of the substrate permittivity (ϵ'_{sub}) and loss (ϵ''_{sub}), as well as of the effective permittivity (ϵ'_{eff}) and loss (ϵ''_{eff}) of the substrate-film composite DR [Figs. 6(c) and 6(d)].

It is seen, that DR parameters (F_R and Q_0) are sufficiently sensitive even to the very thin (22 nm) EuTiO₃ film. The F_R shift resulting from replacing the free substrate by the substrate with a film is small ($2\div 5$ MHz) but still well measurable. It changes with temperature, reflecting temperature dependence of the film permittivity. The change in Q_0 is also large enough ($\sim 10\%\text{--}40\%$) and temperature dependent. The changes in F_R and Q_0 , caused by the 22 nm thick EuTiO₃ film, are similar to that of the composite DR with a

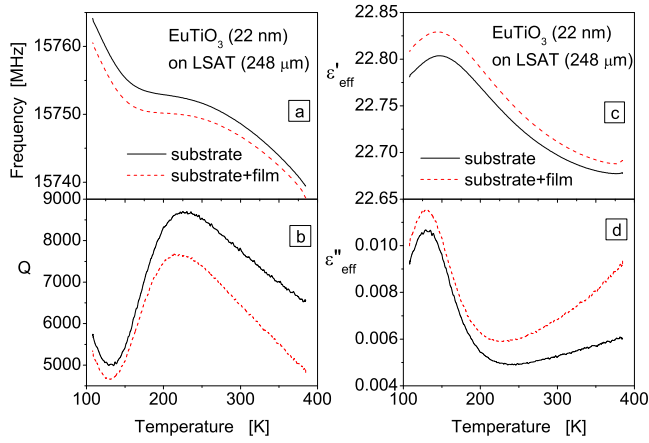


FIG. 6. (Color online) Temperature dependences of the $TE_{01\delta}$ resonance frequency (a), quality factor (b), dielectric permittivity (c), and loss (d) of the LSAT substrate (solid line) and LSAT substrate with $EuTiO_3$ film (dashed line).

base resonator⁷ observed for the much thicker FE films (500–700 nm). It proves the enhanced sensitivity of the thin DR method.

Dielectric parameters of the film (ϵ'_f and ϵ''_f) could be extracted from the ϵ'_{eff} and ϵ''_{eff} accounting for volume fractions of the film and for the fact that electric field is oriented in the plane of both the film and substrate.^{7,10,18} If the film covers the full surface of the substrate (i.e., their effective diameters are equal), ϵ'_{eff} and ϵ''_{eff} can be defined as follows:

$$\epsilon'_{eff} = \epsilon'_{sub} \cdot \frac{L}{L+L_f} + \epsilon'_f \cdot \frac{L_f}{L+L_f}; \quad (2)$$

$$\epsilon''_{eff} = \epsilon''_{sub} \cdot \frac{L}{L+L_f} + \epsilon''_f \cdot \frac{L_f}{L+L_f}, \quad (3)$$

where L and L_f are thickness of the substrate and film respectively. In our case $L \gg L_f$, so the dielectric parameters of the film can be extracted in a simple way

$$\epsilon'_f = \frac{\epsilon'_{eff} \cdot (L+L_f) - \epsilon'_{sub} \cdot L}{L_f} \approx (\epsilon'_{eff} - \epsilon'_{sub}) \cdot \frac{L}{L_f}; \quad (4)$$

$$\epsilon''_f = \frac{\epsilon''_{eff} \cdot (L+L_f) - \epsilon''_{sub} \cdot L}{L_f} \approx (\epsilon''_{eff} - \epsilon''_{sub}) \cdot \frac{L}{L_f}; \quad (5)$$

$$\tan \delta_f = \epsilon''_f / \epsilon'_f. \quad (6)$$

Temperature dependences of dielectric parameters of the $EuTiO_3$ film grown on LSAT substrate (extracted from the data presented in Figs. 6(c) and 6(d)) are shown in Fig. 7. An increase in the permittivity toward low temperatures and hint of its saturation below 120 K evidences incipient FE behavior of the compressively strained $EuTiO_3$ film on LSAT substrate. Second harmonic generation signal as well as infrared reflectance spectra also confirmed¹⁷ that the 0.9% biaxial compressive strain is not sufficient for the induction of FE phase and the film remains incipient FE like in the bulk. The first principles calculations^{16,17} predicted that the compressive strain larger than 1.2% is necessary for induction of ferroelectricity while the LSAT substrate provides only the

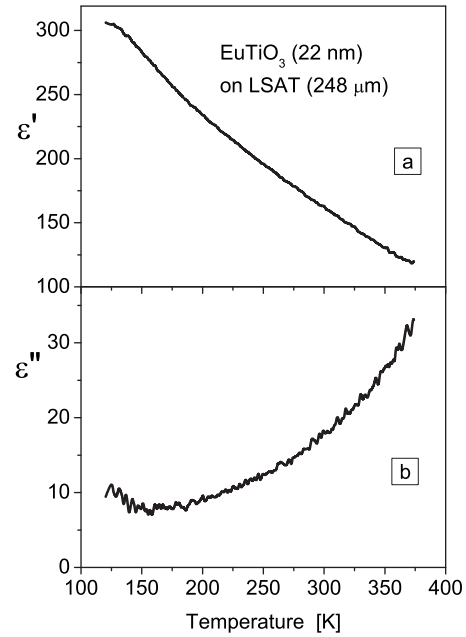


FIG. 7. Temperature dependences of the dielectric permittivity (a) and loss (b) of the 0.9% compressively strained $EuTiO_3$ film grown on (001) LSAT substrate at 15.75 GHz.

0.9% strain. Moreover, the biaxial compressive strain can invoke FE polarization only out of the film plane, therefore permittivity should diverge also out of plane and no significant dielectric anomaly could be seen in the plane of the compressively strained film.

On other hand, first-principle calculations predict that already 0.8% biaxial tensile strain should induce ferroelectricity in $EuTiO_3$ film.^{16,17} In this case the FE polarization should be oriented in the film plane, so a dielectric anomaly should be seen in the in-plane dielectric response near the FE phase transition temperature T_C . Therefore, we investigated a 100 nm thick $EuTiO_3$ film grown on a (110) $DyScO_3$ substrate ($a=b=10$ mm, $L=0.52$ mm) and strained in biaxial tension by 1%. Temperature dependences of the film dielectric parameters (Fig. 8) were obtained from analysis of the $TE_{01\delta}$ resonance mode at 12.15 GHz according to the procedure described above in details for the $EuTiO_3$ film on LSAT substrate. Observed dielectric anomalies reflect the well measurable changes of the DR resonance frequencies and quality factors and are reliable in spite of relatively high possible inaccuracy of the absolute values of dielectric parameters.

Pronounced permittivity and loss maxima at 250 K give an evidence of the strain induced FE phase transition with a polarization in the film plane.¹⁷ Lowest-frequency polar phonon observed in far infrared reflectivity spectra¹⁷ exhibits also anomalous softening near 250 K and its dielectric strength exhibits maximum at the same temperature. Just this FE soft mode is responsible for our observed dielectric anomalies near 250 K. Another pronounced dielectric anomaly is seen near 180 K in Fig. 8. Phonon spectra in Ref. 17 reveal two newly activated phonons near the soft mode frequency, giving the evidence for an antiferrodistortive phase transition (i.e., doubling of unit cell due to a tilting and rotation of oxygen octahedra) near 180 K. However, the activation of new modes itself cannot explain the

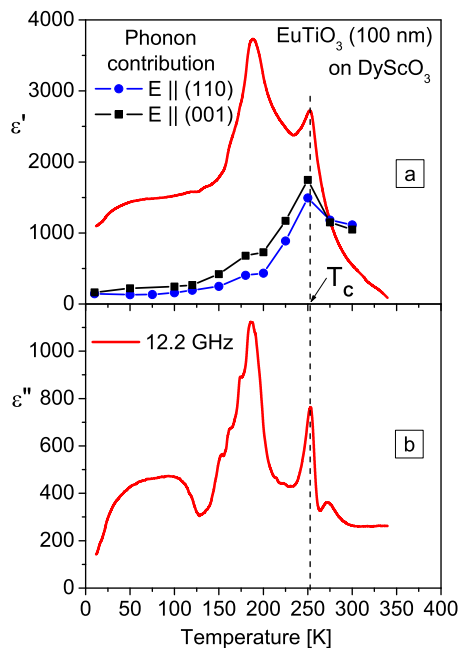


FIG. 8. (Color online) Temperature dependences of the dielectric permittivity (a) and loss (b) of the 1% tensile strained EuTiO_3 film grown on a (110) DyScO_3 substrate at 12.15 GHz. Symbols correspond to the phonon dielectric contribution (Ref. 17).

anomalous increase in permittivity near 180 K; dielectric contribution of the polar phonons does not account for this $\varepsilon'(T)$ maximum.¹⁷ The distinct dielectric peaks near 180 K are probably caused by acoustic emission produced by moving FE and simultaneously ferroelastic domain walls. Such mechanism of the MW dielectric relaxation was proposed by Arlt and Pertsev.^{19,20} On the other hand, if this acoustic emission is influenced by the antiferrodistortive phase transition, the dielectric peaks could be related to the transition temperature.

Successful characterization of the ultrathin (22 and 100 nm) EuTiO_3 films with significantly different dielectric properties evidences efficiency of the thin DR method. Application of the method to the film with permittivity from $\varepsilon'_f=100$ to $\varepsilon'_f=4000$ was demonstrated. The monotonic temperature dependence (Fig. 7), as well as distinct anomalies (Fig. 8) of the film dielectric parameters can be revealed. Sensitivity of the method to the value of the film permittivity was estimated using the ANSOFT HFSS software¹¹ for different film thicknesses. In the case of a thin substrate, change of the DR resonance frequency caused by the film permittivity increase from $\varepsilon'_f=100$ to $\varepsilon'_f=600$ reaches tens or even hundreds of MHz for the 100–1000 nm thick films (Fig. 9). High sensitivity to the film dielectric parameters proves that the thin DR method is a promising new tool for MW characterization of the high-permittivity thin films. The method requires no electrode deposition; the setup and measurement procedure is quite simple and traditional for MW materials. The main requirement is a precise geometry of the substrates, identical thickness, and diameter of the substrates with and without film.

IV. CONCLUSIONS

A thin DR consisting of the dielectric substrate and thin film deposited upon it is proposed to be used for MW char-

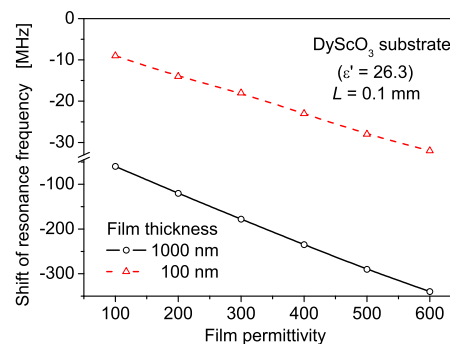


FIG. 9. (Color online) Calculated shift of the $\text{TE}_{01\delta}$ resonance frequency of rectangular (110) DyScO_3 substrates ($a=b=10$ mm, $L=0.1$ mm) with a 1000 nm (solid line) and 100 nm (dashed line) thick films in the shielding cavity comparatively to that of the substrate without film dependent on the film permittivity.

acterization and dielectric parameters measurement of the high-permittivity thin films without electrodes. The $\text{TE}_{01\delta}$ resonance mode was excited and identified in thin (down to 0.1 mm) rectangular- or disk-shaped low-loss dielectric substrates ($D \sim 10$ mm) with permittivity $\varepsilon' \geq 10$ inserted into the cylindrical shielding cavity or rectangular waveguide. The in-plane dielectric permittivity and losses of alumina, DyScO_3 , SmScO_3 , and LSAT substrates were measured at 10–18 GHz. The substrate thickness optimal for the deposited thin film characterization varies from 0.65–0.85 mm for alumina or sapphire substrates to 0.2–0.3 mm for DyScO_3 substrates depending on the substrate permittivity. Efficiency of the method and high sensitivity of the thin DR to the film parameters was demonstrated by characterizing ultrathin strained EuTiO_3 films. A 22 nm thick EuTiO_3 film grown on a (100) LSAT substrate and strained in biaxial compression by 0.9% exhibited an increase in MW permittivity at low temperatures consistent with it being an incipient FE; no strain-induced FE phase transition was seen above 100 K. In contrast, a 100 nm thick EuTiO_3 film grown on a (110) DyScO_3 substrate and strained in biaxial tension by 1% showed two peaks as a function of temperature in MW permittivity and loss. These peaks correspond to a strain-induced FE phase transition near 250 K and to the FE/ferroelastic domain wall motion near the antiferrodistortive phase transition temperature 180 K. The above mentioned results prove high capability of the thin DR method in MW dielectric investigation of the electrode-free ultrathin high-permittivity films.

ACKNOWLEDGMENTS

The financial support by the Czech Science Foundation (Project Nos. 202/09/0682, AVOZ10100520) and by the National Science Foundation (Grant No. DMR-0820404) are gratefully acknowledged.

¹O. G. Vendik, E. K. Hollmann, A. B. Kozyrev, and A. M. Prudan, *J. Supercond.* **12**, 325 (1999).

²A. K. Tagantsev, V. O. Sherman, K. F. Astafiev, J. Venkatesh, and N. Setter, *J. Electroceram.* **11**, 5 (2003).

³Y. M. Poplavko and N.-I. Cho, *Semicond. Sci. Technol.* **14**, 961 (1999).

⁴A. K. Tagantsev and G. Gerra, *J. Appl. Phys.* **100**, 051607 (2006).

⁵K. Sudheendran, D. Pamu, M. Ghanashyam Krishna, and K. C. James

- Raju, *Measurement* **43**, 556 (2010).
- ⁶B. Kim, V. Kazmirenko, Y. Prokopenko, Y. Poplavko, and S. Baik, *Meas. Sci. Technol.* **16**, 1792 (2005).
- ⁷V. Bovtun, S. Veljko, A. Axelsson, S. Kamba, N. Alford, and J. Petzelt, *Integr. Ferroelectr.* **98**, 53 (2008).
- ⁸J. Krupka, K. Derzakowski, B. Riddle, and J. Baker-Jarvis, *Meas. Sci. Technol.* **9**, 1751 (1998).
- ⁹J. Krupka, *Meas. Sci. Technol.* **17**, R55 (2006).
- ¹⁰V. G. Tsykalov, V. M. Pashkov, and V. P. Bovtun, Dielectrics and Semiconductors. Republican interdepartmental scientific and technical article collection, **18**, 7 (1980) (in Russian).
- ¹¹<http://www.ansoft.com/products/hf/hfss/>
- ¹²B. C. Chakoumakos, D. G. Schlom, M. Urbanik, and J. Luine, *J. Appl. Phys.* **83**, 1979 (1998).
- ¹³D. G. Schlom, L.-Q. Chen, Ch.-B. Eom, K. M. Rabe, S. K. Streifer, and J. M. Triscone, *Annu. Rev. Mater. Res.* **37**, 589 (2007).
- ¹⁴D. Nuzhnyy, J. Petzelt, S. Kamba, P. Kužel, C. Kadlec, V. Bovtun, M. Kempa, J. Schubert, C. M. Brooks, and D. G. Schlom, *Appl. Phys. Lett.* **95**, 232902 (2009).
- ¹⁵T. Katsufuji and H. Takagi, *Phys. Rev. B* **64**, 054415 (2001).
- ¹⁶C. J. Fennie and K. M. Rabe, *Phys. Rev. Lett.* **97**, 267602 (2006).
- ¹⁷J. H. Lee, L. Fang, E. Vlahos, X. Ke, Y. W. Jung, L. Fitting Kourkoutis, J. W. Kim, P. J. Ryan, T. Heeg, M. Roeckerath, V. Goian, M. Bernhagen, R. Uecker, P. C. Hammel, K. M. Rabe, S. Kamba, J. Schubert, J. W. Freeland, D. A. Muller, C. J. Fennie, P. Schiffer, V. Gopalan, E. Johnston-Halperin, and D. G. Schlom, *Nature (London)* **466**, 954 (2010).
- ¹⁸V. G. Tsykalov, V. M. Pashkov, and V. P. Bovtun, Dielectrics and Semiconductors **15**, 48 (1979) (in Russian).
- ¹⁹G. Arlt, U. Böttger, and S. Witte, *Ann. Phys.* **506**, 578 (1994).
- ²⁰N. A. Pertsev, G. Arlt, and A. G. Zembilgotov, *Phys. Rev. Lett.* **76**, 1364 (1996).